

# Cloud microphysical process in single-layer arctic stratus during MPACE

Gong Zhang<sup>1</sup>, Greg McFarquhar<sup>1</sup>, Johannes Verlinde<sup>2</sup>, Michael Poellot<sup>3</sup>, Greg Kok<sup>4</sup>, Edwin Eloranta<sup>5</sup>, Paul DeMott<sup>6</sup>, Tony Prenni<sup>6</sup> and Andrew Heymsfield<sup>7</sup>

<sup>1</sup> University of Illinois <sup>2</sup> Pennsylvania State University <sup>3</sup> University of North Dakota <sup>4</sup> Droplet Measurement Technologies

<sup>5</sup> University of Wisconsin <sup>6</sup> Colorado State University <sup>7</sup> National Center for Atmospheric Research

## 1 Arctic boundary single-layer stratus

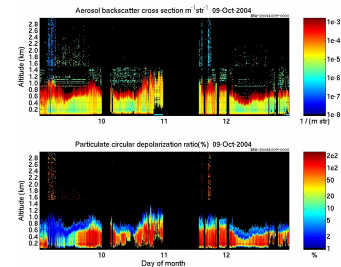


FIG 1 Backscatter intensity and depolarization ratio measured by Wisconsin HSRL Lidar in Barrow, AK. During MPACE, single-layer arctic stratus was observed from Oct 09 2004 to Oct 12 2004.

## 2 Vertical cloud structure

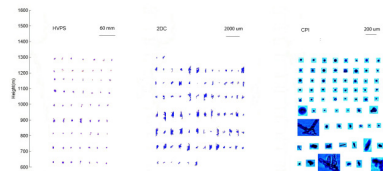


FIG 2 Example of selected HVPS (left), 2DC (middle) and CPI (right) images acquired for spiral flow between 2140 and 2147 on 10 October 2004 through a single-layer stratus. Smaller spherical images near cloud top (CPI) are small drizzle or supercooled drops. Larger ice crystal images show dominance of irregular and rimed crystal shapes throughout cloud and precipitating beneath cloud base.

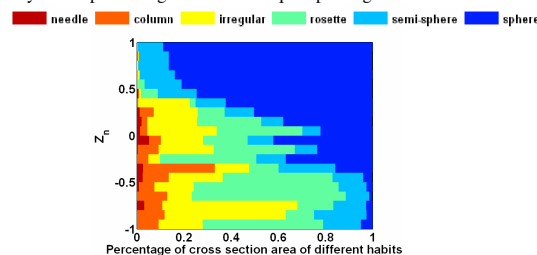


FIG 3 Normalized fractional contribution of different habits to the total cross-sectional area as a function of normalized cloud altitude,  $z_n$ , derived from all spirals flow through single-layer Arctic stratus. Habit fractions derived from automated habit recognition scheme applied to CPI data, cross-sectional area derived from analysis of CPI images.  $z_n$  is distance above cloud base divided by the cloud thickness.

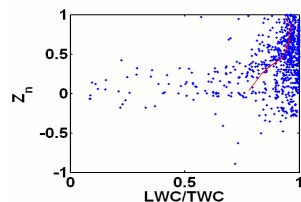


FIG 4 Variation of LWC/TWC as function of  $z_n$  derived for all spirals flow through single-layer mixed-phase clouds. Here LWC (liquid water content) is measured by a King probe. TWC (total water content) is calculated by adding LWC and IWC, where IWC is calculated by using size distribution data and m-D relation constrained to best match IWC measured by CVI in ice-phase clouds.

## 3 Cloud microphysical process

### 3.a Condensational growth of water droplets

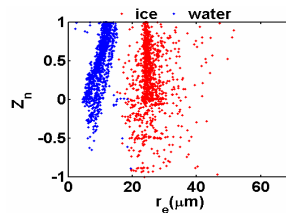


FIG 5 Vertical variation of  $r_{ew}$  (effective radius of water droplets) and  $r_{ei}$  (effective radius of ice crystals). Increase of  $r_{ew}$  with height in cloud is seen whereas  $r_{ei}$  is less correlated with  $z_n$ .

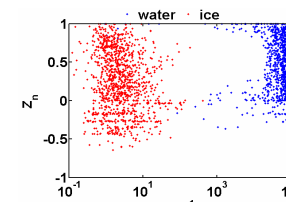


FIG 6 Vertical variation of  $N_w$  (number concentration of water droplets) and  $N_i$  (number concentration of ice crystals with  $D>53 \mu\text{m}$ ). On average,  $N_w$  changed by only 8% between  $z_n$  of 0.1 and 0.8.

The increase of  $r_{ew}$  with  $z_n$  and relatively constant  $N_w$  with  $z_n$  suggest condensational growth of water droplets and additional nucleation did not take place inside the cloud.

### 3.b Ice enhancement

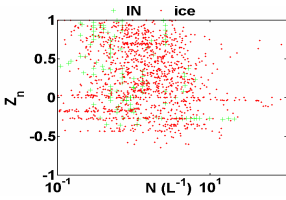


FIG 7 Vertical variation of IN (number concentration of ice nucleus) and  $N_i$ .  $N_i$  is 10 times bigger than IN, suggesting secondary ice crystal production processes are occurring.

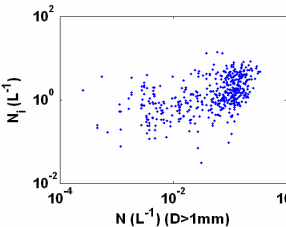


FIG 8 number concentration of large ice crystals ( $D>1\text{mm}$ ) versus  $N_i$ .  $N_i$  tends to increase with large ice crystal number concentration. As  $N_i$  is dominated by the contribution from ice crystals with  $D>1\text{mm}$ , Fig 8 indicates number concentration of large ice crystals and small ice crystals are positively correlated.

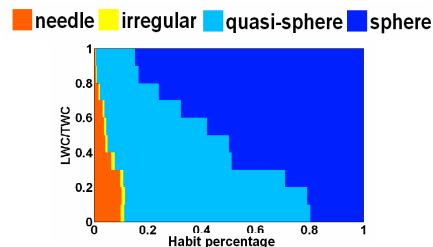


FIG 9 Variation of cloud particle ( $15<D<60 \mu\text{m}$ ) habit distribution with LWC/TWC. More spherical and less quasi-spherical particles with increasing LWC/TWC.

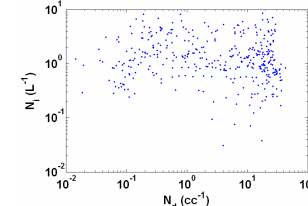


FIG 10  $N_d$  (number concentration of spherical droplets with  $D>23 \mu\text{m}$ ) versus  $N_i$ . Here  $N_d$  calculated using FSSP distribution and the relationship between spherical droplets and LWC/TWC shown in FIG 9. Unlike previous work (Rangno and Hobbs 2001),  $N_i$  doesn't show strong dependence on  $N_d$ . This indicates riming-splintering process may not be significant in these arctic stratus clouds.

### 3.c Ice particle growth

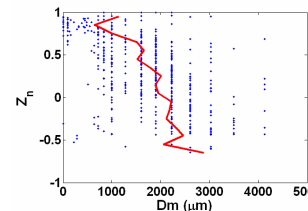


FIG 11 Variation of  $D_m$  as function of  $z_n$ .  $D_m$  decreases with  $z_n$ . This indicates ice crystal has bigger max dimension with decreasing height.

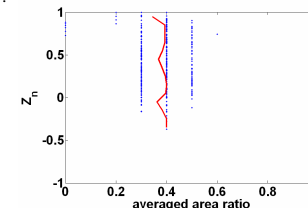


FIG 12 Variation of averaged area ratio as function of  $z_n$ . Area ratio almost remains constant.

## 4. Conclusions

■ Effective radius of water drops ( $r_{ew}$ ) increases with  $z_n$  while total number of water drops ( $N_w$ ) is not strongly correlated with  $z_n$ . This indicates condensational growth of water droplets.

■  $N_i$  concentrations too large to be explained by primary nucleation mechanisms.  $N_i$  tends to increase with number concentration of ice crystals with  $D>1\text{mm}$  while it doesn't show strong dependence on  $N_d$ .

■ Ice crystals tends to be bigger with decreasing height while having the same area ratio.

## 5. Acknowledgments

This research was supported by DOE ARM under contract number DE-FG02-00ER62913.